International Journal of Fatigue 31 (2009) 1095–1101

Contents lists available at ScienceDirect

International Journal of Fatigue

journal homepage: www.elsevier.com/locate/ijfatigue

# Comparison of different setups for fatigue testing of thin composite laminates in bending

I. De Baere *, W. Van Paepegem, J. Degrieck

*Department of Mechanical Construction and Production, Faculty of Engineering, Ghent University. Sint-Pietersnieuwstraat 41, B-9000 Gent, Belgium*

ARTICLE INFO

*Article history:*
Received 11 February 2008
Received in revised form 14 May 2008
Accepted 14 May 2008
Available online 27 May 2008

*Keywords:*
Clamped bending
Composites
Carbon fibre
PPS

ABSTRACT

After developing a damage model, validation of this model is a necessity. This validation should preferably be done under loading conditions which are different from the ones used for the development of the model.

This study investigates whether a special design of a bending setup is suited for the mechanical testing of thin fibre-reinforced composites with a low bending stiffness and the validation of fatigue material models, developed in uni-axial loading conditions. First, the disadvantages of a three-point bending setup for thin laminates are commented on. Then, a four-point bending setup is discussed, for which interestingly enough, the finite-element model can be simplified. Clamped supports are added to decrease the midspan displacement. This is followed by the discussion of the clamped three-point bending setup.

It may be concluded that the clamped three-point bending setup is very promising for experimental work, since it increases the measured loads and decreases the midspan displacement with respect to the regular three-point bending setup, although further modification of the setup is necessary to avoid slipping in the grips.

The material used for this study was a carbon fabric-reinforced polyphenylene sulphide.



## 1. Introduction

The vast majority of fatigue tests on fibre-reinforced composites are performed in uni-axial tension/tension or tension/compression fatigue [1–5]. These tests are accepted by international standards (ASTM D3479) and provide the S–N data for the tested material.

Although bending fatigue tests are not widely accepted as a standard, they are used a lot for research purposes [6–8]. They do have some important advantages as well: (i) bending loads often occur in in-service loading conditions, (ii) there are no problems with buckling, compared to tension/compression fatigue, and (iii) the required forces are much smaller. To evaluate the stiffness degradation and damage growth in the fibre-reinforced laminate, the hysteresis loop of one loading cycle can be measured. In case of three-point bending fatigue, the history of bending force versus midspan displacement is recorded.

In [9], the authors examined a standard three-point bending setup for thin composite laminates. It was concluded that, despite the interesting loading conditions in the setup, this setup was not suited for this purpose because of the following two reasons: (i) the midspan displacement of the specimen was very large, limiting the test frequency in the fatigue test and causing extra difficulties in interpreting hysteresis loops, because of the occurring friction on the supports and (ii) the simulation of this setup is difficult, since the supports must be modelled in order to take the friction into account and the simulations require a lot of time, because of convergence problems in the contact conditions at the supports.

This study investigates whether a modified bending setup may be used for the validation of damage models. First, the disadvantages of a modified three-point bending setup with rotating supports are commented on. Then, a four-point bending setup is discussed, because its loading conditions allow easy finite-element modelling. A clamped four-point bending setup is then discussed, since the clamping would reduce the midspan displacements. This is followed by a clamped three-point bending setup. Finally, some conclusions are drawn. In the next paragraph, the used composite material and tensile machine are discussed.

## 2. Materials and methods

### 2.1. Composite material

The material used for the experiments was a five-harness satin-weave carbon fabric-reinforced polyphenylene sulphide (PPS). The carbon PPS plates were hot pressed, one stacking sequence was used for this study, namely $[(0°, 90°)]_{4s}$ where (0°, 90°) represents one layer of fabric. The in-plane elastic properties and the tensile

* Corresponding author. Tel.: +32 9 264 32 55; fax: +32 9 264 35 87.
*E-mail address:* Ives.DeBaere@UGent.be (I. De Baere).

0142-1123/$ - see front matter © 2008 Elsevier Ltd. All rights reserved.
doi:10.1016/j.ijfatigue.2008.05.011

**Table 1**
Elastic and strength properties of the CETEX® material

| | | | |
|---|---|---|---|
| $E_{11}$ (GPa) | 56.0 | $X_T$ (MPa) | 736 |
| $E_{22}$ (GPa) | 57.0 | $\varepsilon_{11}^{ult}$ (–) | 0.011 |
| $\nu_{12}$ (–) | 0.033 | $Y_T$ (MPa) | 754.0 |
| $G_{12}$ (GPa) | 4.175 | $\varepsilon_{22}^{ult}$ (–) | 0.013 |
| | | $S_T$ (MPa) | 110.0 |

strength properties are listed in Table 1 [11]. This material was supplied to us by Ten Cate Advanced Composites (The Netherlands).

The test coupons were sawn with a water-cooled diamond saw.

### 2.2. Equipment

All bending tests were performed on a servo-hydraulic INSTRON 1342 servo-hydraulic machine with a FastTrack 8800 digital controller. For the registration of the data, a combination of a National Instruments DAQpad 6052E for fireWire, IEEE 1394 and the SCB-68 pin shielded connecter were used. The load and displacement, given by the FastTrack controller, were sampled on the same time basis.

## 3. Experiments and discussion

### 3.1. The modified three-point bending setup with rotating supports

In [10], the authors had already examined whether the standard three-point bending setup was suited for testing thin composite laminates. A special setup with rotating supports was presented (Fig. 1a), to avoid impacting of the indenter on the specimen in displacement-controlled fatigue tests, due to permanent deformation. Furthermore, the rotating of the support diminishes the effect of friction on the hysteresis loops.

However, two major problems occurred during the experiments: (i) the finite-element modelling (Fig. 1b) of the setup was problematic, because the (rotating) supports needed to be modelled to have the effect of friction on the supports and the simulations took a lot of computation time and (ii) the midspan displacements were large, limiting the test frequency of the fatigue test.

### 3.2. The four-point bending setup

Contrary to the three-point bending setup presented in the previous paragraph, a four-point bending setup has a more interesting load distribution for modelling (Fig. 2).

The area between the two indenting rolls has a constant bending moment equal to $-Fa/2$ and no transverse force. As a result, the finite-element modelling of a load controlled test is very straightforward, only the section between the two indenting rolls must be modelled and a corresponding moment must be applied.

However, problems arose during the experimental assessment of this setup. Fig. 3a shows the used geometry for these bending experiments; for the span, values of 30, 40 and 50 mm were chosen to see its effect on the force–displacement curves.

However, for the experiments with a span of 40 and 50 mm, the specimen could not be bent until fracture, because of limitations in the setup. This is illustrated in Fig. 3b. Because of the large midspan displacements, the mounting mechanism of the indenting rolls makes contact with the specimen, instead of the indenting rolls.

For a 30 mm span, failure was reached right before the unwanted contact established. For comparison purposes, another loading and unloading experiment was done on the 30 mm span setup with a maximum load of 90% of the failure load from the previous test. The force–displacement curves for the three setups are shown in Fig. 4a; the 'span' is the distance between the indenting rolls, as illustrated in Fig. 3a. It must be noticed that, even for the 30 mm span, the loads are relatively low and the midspan displacements are quite high, again limiting the maximum frequency of a fatigue test. It must be noted that quite large hysteresis loops are visible, but very limited permanent deformation is visible. The hys-

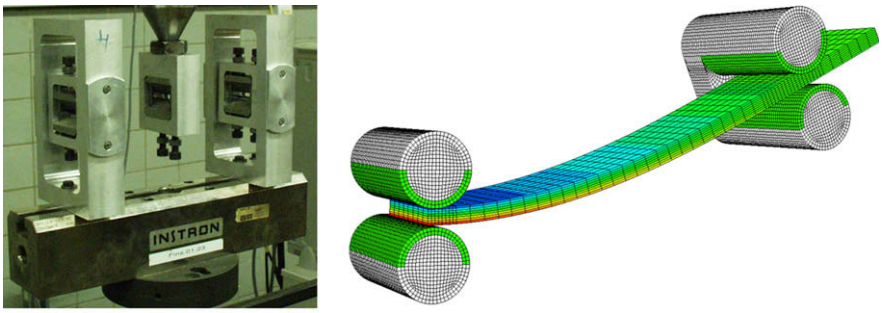


**Fig. 1.** The modified three-point bending setup with rotating supports [10].

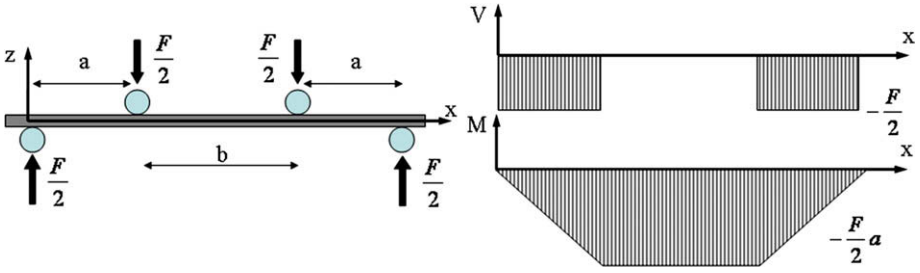


**Fig. 2.** Illustration of the occurring loads in a four-point bending setup.

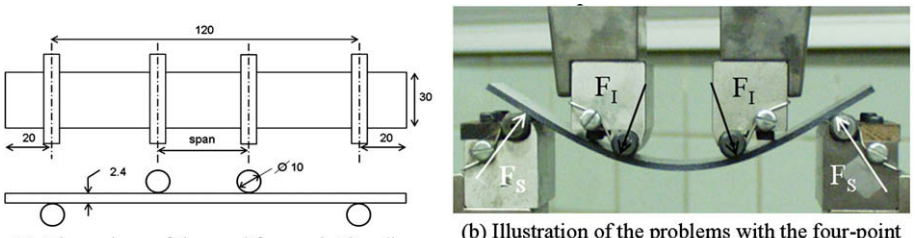


(a) Dimensions of the used four-point bending coupon in millimetres.

(b) Illustration of the problems with the four-point bending setup; the high midspan displacement causes the reaction forces to deviate from the vertical axis

**Fig. 3.** Four-point bending setup.

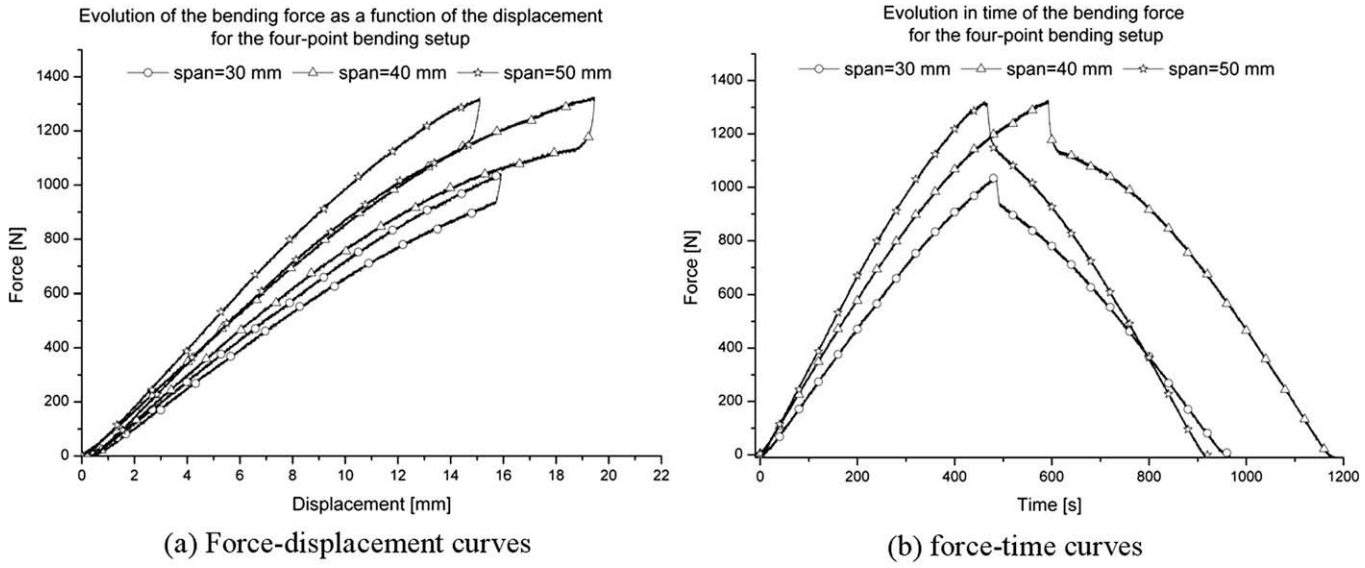


(a) Force-displacement curves

(b) force-time curves

**Fig. 4.** Hysteresis loops in the four-point bending experiments.

teresis loops, however, are entirely due to the friction on the supports, as was documented in [9]. This can be seen in the evolution of the force as a function of time in Fig. 4b, where the sudden drop is visible.

Another major set back is illustrated in Fig. 3b. Since thin laminates are tested, the midspan displacements become so large that the occurring loads are no longer given by Fig. 2. Since $F_S$ and $F_I$ are perpendicular to the (bent) surface of the specimen, they are no longer vertical, introducing normal forces in the specimen. Therefore, the simple finite-element model described above is no longer valid and the entire setup must be modelled and a geometrically non-linear calculation must be performed. As a result, the main advantage of this setup over the standard three-point bending, namely the straight-forward numerical modelling, is lost because the midspan displacement of the thin laminates under study is too large.

### 3.3. The clamped four-point bending setup

In order to have higher forces for lower displacements, the specimen is clamped at both ends, inducing membrane stresses. However, this compromises the easy modelling in finite-element software, since the membrane stresses cannot be determined in an analytical formula and hence, the entire setup (using symmetry) must be modelled. A first experiment, however, yielded another problem: the specimen failed at the clamped ends. This, however, could be expected, since simple beam theory also yields that the bending moment at the clamps, using the dimensions from Fig. 2, is given by [12]

$$M = F\frac{l^2 - b^2}{4l} \tag{1}$$

where $l$ equals $a + b$. The (constant) moment in the area between the indenters is given by [12]

$$M^* = F\frac{(l-b)^2}{4l} \tag{2}$$

Solving $M^* > M$ yields $b > l$, which of course is impossible. However, the experiment indeed yielded a higher bending load for a lower midspan displacement; the specimen failed at 2636 N with corresponding midspan displacement of 8.3 mm.

### 3.4. The clamped three-point bending setup

Because of the good results of the clamped edges in the previous paragraph, the same principle is used on a three-point bending setup. The used setup is illustrated in Fig. 5a, the dimensions of the coupons used for these bending experiments are shown in Fig. 5b, all dimensions are in millimetres.

Preliminary tests had shown that the two clamps tended to slide inwards due to the high membrane stresses. Therefore, a small piece of aluminium was placed between the two grips, at the exact width, preventing them from sliding inwards. The results of a few quasi-static tests are shown in Fig. 6, the corresponding

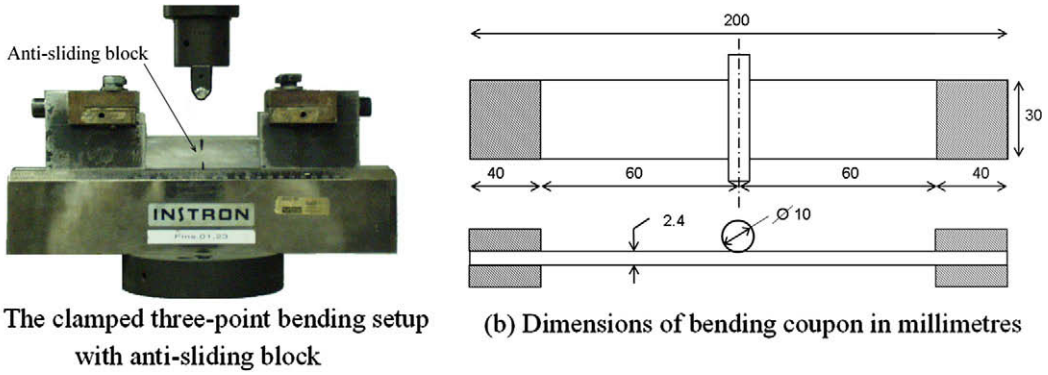


(a) The clamped three-point bending setup with anti-sliding block

(b) Dimensions of bending coupon in millimetres

**Fig. 5.** The clamped three-point bending setup.

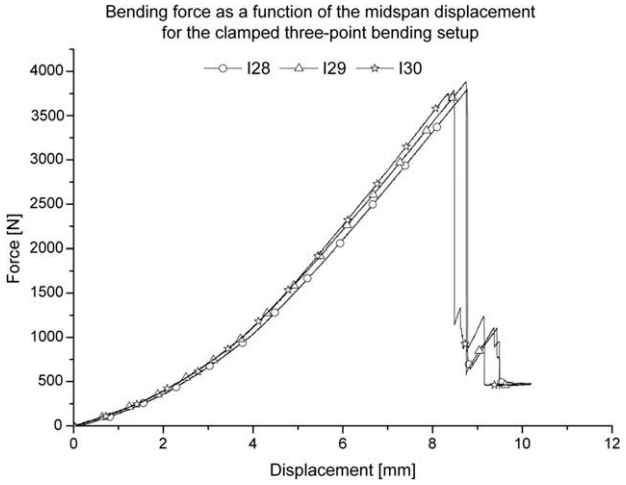


**Fig. 6.** Force-displacement curves of the quasi-static test with the clamped three-point bending setup.

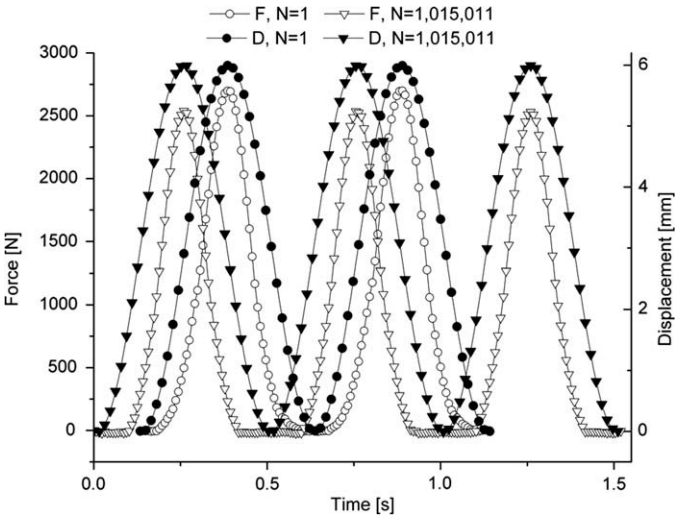


**Fig. 7.** Force and displacement as a function of time for the first and last measurement.

displacement speed was 2 mm/min. It may be remarked that the results are very reproducible, there is only a limited difference, due to scatter on the results. Furthermore, high forces for low displacements are achieved; the loads are four times higher at failure, for less than half the displacement when compared with the standard three-point bending setup [10]. As can be seen in Fig. 6, the force at failure is about 3.8 kN. This, however, is still significantly lower than the failure force in a uni-axial tensile test, which is about 52.6 kN for a specimen with a thickness of 2.4 mm and a width of 30 mm. Therefore, the third advantage, mentioned in Section 1, is valid.

Because of the improvements with respect to the standard three-point setup, some fatigue tests have been done. During those tests, it was noticed that after a few hundred cycles, the indenter lost contact over a certain period of time. This is illustrated in Fig. 7, which shows the evolution of the bending force and the displacement as a function of time for a few cycles from a displacement-controlled test with amplitude of 6 mm and a frequency of 2 Hz. It must be noted that for the last depicted cycle (1,015,011 cycles) the load remains zero for a certain period of time, although the displacement varies. This means that the indenter looses contact during cycling. The latter may be caused by permanent deformation or slipping inside the grips.

Therefore, small markings were placed on the specimen next to the clamps to verify if the specimen slips out of the grips. It was noticed that the specimen indeed slipped over a very limited distance, circa 0.5 mm, because of the very high membrane stresses.

Of course, in uni-axial testing, slippage in the grips also occurs, because of the higher forces. However, the slippage does not affect the eventual results, since the slippage has no influence on the longitudinal force and since the longitudinal strain should be measured with strain gauges or extensometer, rather than calculated using the displacement and the span, the strain also is not influenced. Therefore, using serrated grips and applying sufficient pressure is enough to limit the slippage in uni-axial testing. These precautions, however, were already implemented in the clamped three-point bending setup. Since the slippage does influence the actual measurement, other precautions must be taken. Possibilities are to use an additional (hydraulic) actuator to compensate the sliding by readjusting the position of the grips, to use hydraulic gripping to further increase the gripping pressure or to use bolts through the specimen, ensuring that this does not advance preliminary failure. This sliding, however, would explain the loss of contact in Fig. 7, although permanent deformation may not be neglected.

Despite the little sliding, already a few fatigue tests were performed to establish the outer boundaries, varying from failure after a few dozen cycles to infinite fatigue life. All these preliminary tests were done with a loading frequency of 2 Hz in displacement-controlled mode. The tests had displacement amplitude of 6, 7 and 7.5 mm. The first experiment was stopped after 1,015,010 cycles and it was considered to be infinite life, the specimen did not break and showed very limited permanent

deformation. Since the load distribution in the bending setup is pure tension or compression along the fibre, but no shear, this amount of permanent deformation is consistent with the results from the uni-axial fatigue tests on the $[(0°, 90°)]_{4s}$ stacking sequence. The latter also showed only very limited permanent deformation. The run-in of this test is shown in Fig. 8; it should be noted that hysteresis loops occur and that the indenter makes contact during the entire cycle, since the force does not remain zero over a certain range of the displacement. This means that sliding in the grips accumulates slowly during fatigue cycling, rather than suddenly during the run-in. It should be mentioned that in the quasi-static tests sliding did happen, but the static displacements at failure were 50% higher than the displacement amplitudes in fatigue (9 mm at failure versus 6 mm after the run-in). This would mean that sliding starts either after a certain number of cycles at low amplitude or after one cycle with a larger amplitude.

Fig. 9 illustrates the evolution of the maximum, minimum and average value of the bending force throughout the fatigue experiment. There is a slight decrease, but this is more likely the result of sliding in the grips than of stiffness degradation, since the uni-axial tests also did not yield any stiffness degradation.

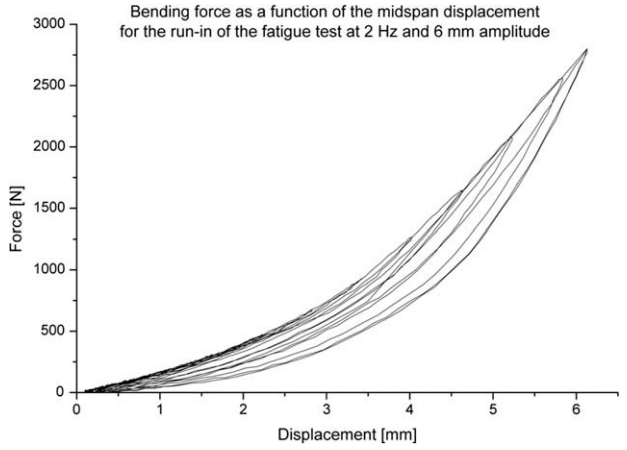


**Fig. 8.** Force as a function of the displacement for the run-in of the 6 mm fatigue test.

The specimen from the fatigue test with 7 mm amplitude failed in the mid section after about 200 cycles and the 7.5 mm amplitude caused failure to occur during the run-in of the test, as is illustrated in Fig. 10.

As can be seen, the specimen failed right before it reached the maximum amplitude. It can also be noticed in Fig. 10 that for displacements higher than 6 mm, the sliding gradually begins; the cycle that reaches 5.75 mm has zero force for zero displacement, but the next cycle, which reaches 6.25 mm, there is already a short moment in time where the force remains zero. This again suggests that sliding either starts after a number of cycles at low amplitude or after few cycles with large amplitudes.

Finally, it should be remarked that the amplitude range, varying from infinite lifetime to failure in a few dozen cycles is very narrow, only 1.5 mm of amplitude change is sufficient. Of course, more tests should be performed to validate this conclusion, but again, this is consistent with the results found from uni-axial fatigue tests, where also only a narrow load range was found from infinite fatigue life to almost immediate failure.

To investigate which fraction of the bending force is due to the membrane stresses and how much comes from the bending itself, finite-element simulations have been done using ABAQUS™ standard. Using the symmetry of the setup, only a quarter was modelled in three-dimensional quadratic brick elements with reduced integration, C3D20R; the size of the elements was 1 mm to have a dense mesh. This is illustrated in Fig. 11.

In a first simulation, the gripped section of the specimen was not allowed to move inwards (three-dimensional clamped). In a second simulation, the gripped section could slide freely (three-dimensional sliding). The boundary conditions for these simulations are given in Table 2; since three-dimensional elements are used, there are no rotational degrees of freedom. For the bending load, a displacement $U_2 = 10$ mm was enforced on the reference point of the indenting roll, $R_P$.

To assess whether it is necessary to perform three-dimensional calculations, the same simulations were redone, but with simple beam theory (one-dimensional). For this simulation, no symmetry was used, so the entire specimen was modelled, using a three node quadratic beam element in space, B32 with a size of 2 mm (see Fig. 12).

For points A and C, all movement is restricted, which means that $U_1 = U_2 = U_3 = 0$; $\alpha_1 = \alpha_2 = \alpha_3 = 0$; a vertical displacement $U_2 = 10$ mm enforced on point B.

Of course, for both the three- as the one-dimensional simulation, a geometrical non-linear analysis was performed. The

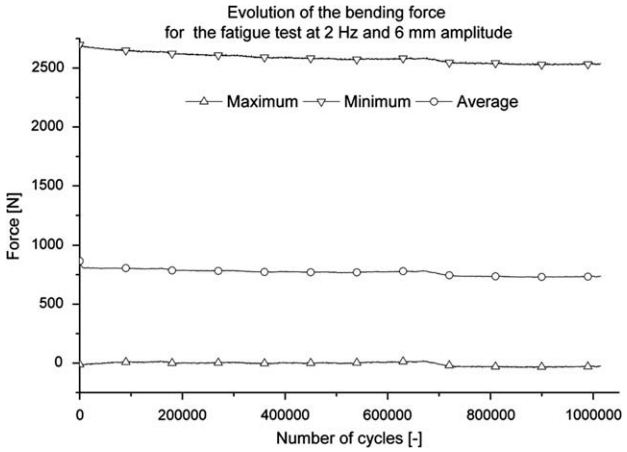


**Fig. 9.** Evolution of the maximum, minimum and average value of the force during the 6 mm fatigue test.

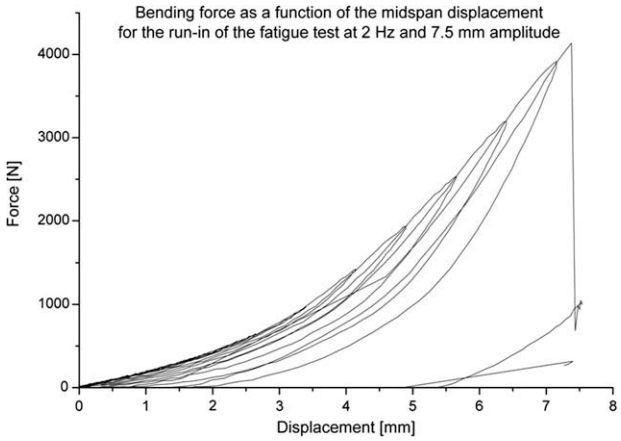


**Fig. 10.** Force as a function of the displacement for the run-in of the 7.5 mm fatigue test, illustrating the failure.

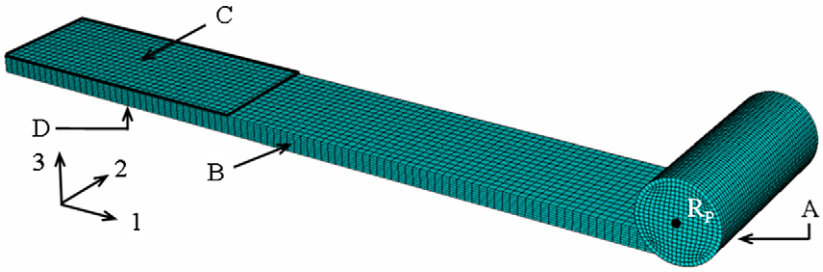


**Fig. 11.** Finite-element model of the clamped three-point bending setup.

**Table 2**
Used boundary conditions for the three-dimensional simulations

| Simulation | Face A | Face B | Face C | Face D |
|---|---|---|---|---|
| Three-dimensional clamped | $U_1 = 0$ | $U_2 = 0$ | $U_1 = U_2 = 0$ | $U_1 = U_2 = U_3 = 0$ |
| Three-dimensional sliding | $U_1 = 0$ | $U_2 = 0$ | $U_2 = 0$ | $U_2 = U_3 = 0$ |

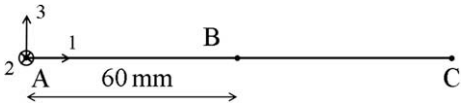


**Fig. 12.** Illustration of the one-dimensional model of the clamped setup. No symmetry is used.

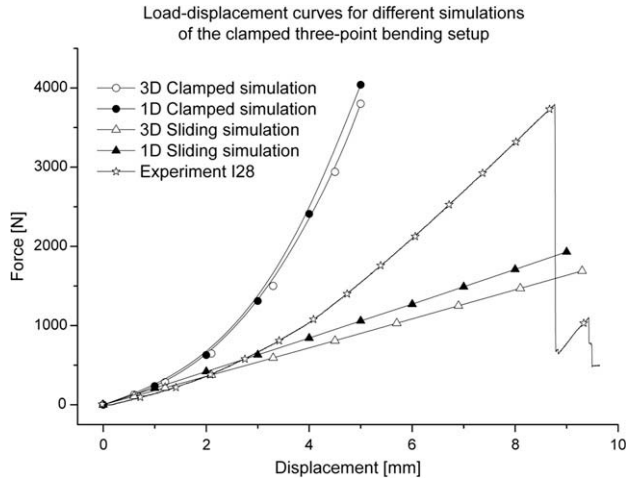


**Fig. 13.** Different force–displacement curves for the simulations of the clamped setup.

implemented material data is the same as in Table 1. The results of these simulations are depicted in Fig. 13.

First of all, it must be noted that if sliding in the grips is allowed, the force decreases significantly for a given displacement. Since there was a little sliding in the experiment (I28), the corresponding curve lies closer to the simulation where sliding was allowed. Again this emphasizes the need for a non-sliding setup.

It can also be remarked that the simple elastic beam theory does not differ a lot from the three-dimensional analysis. The latter is very useful for fatigue simulations, with or without damage models, since a one-dimensional calculation with a linear material model is done in a matter of seconds, whereas the three-dimensional analysis takes a few hours to complete because of the dense mesh needed for accurate results.

Also, it is very easy to obtain values of the bending moments, longitudinal and transverse forces from the one-dimensional analysis, whereas for the three-dimensional simulations, these values need to be calculated manually from the stress distributions. Fig. 14 gives an overview of the values of the bending moment, the transverse force and the longitudinal force for the one-dimensional analysis, for a displacement of 9 mm, corresponding to the fracture of the experiment. The forces have been rescaled to have a clear image; the scaling factor differs for both graphs.

Because of the clamping, very high longitudinal forces are imposed. For the sliding setup, the force only becomes 200 N, whereas for the clamped specimen, the force is almost 47,800 N, which is almost 250 times higher. For the sliding setup, the evolution of the bending moment and transverse force is about the same as with the standard three-point bending setup. By inhibiting the ends of the specimen to slide inwards, the maximum bending moment almost doubles, whereas the transverse force in the centre of

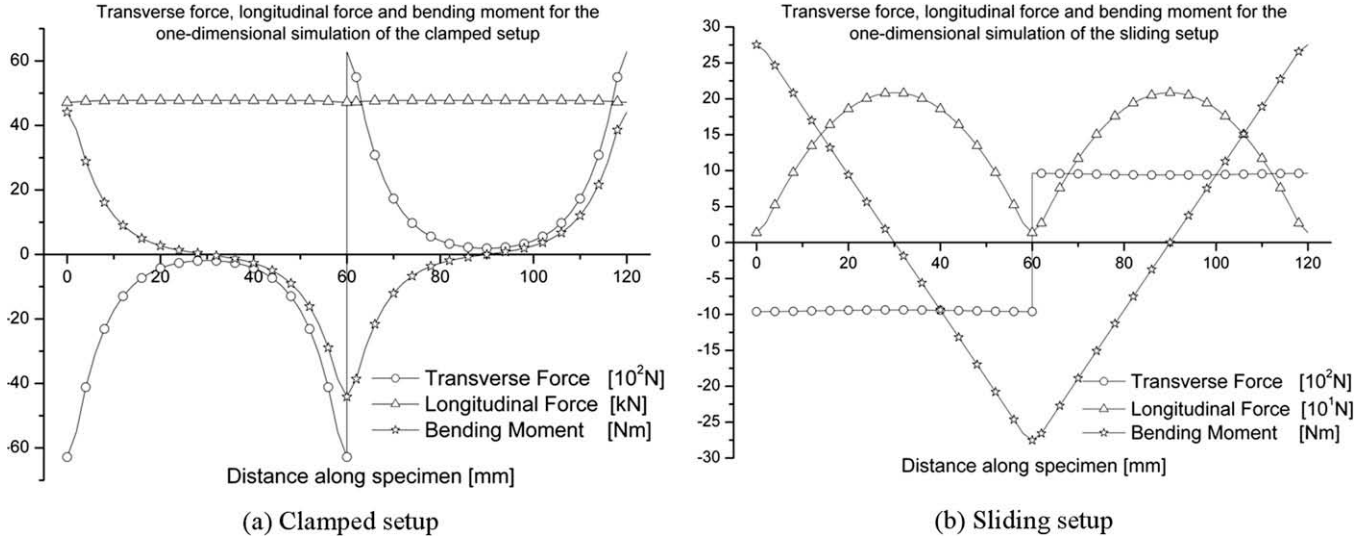


**Fig. 14.** Evolution of the longitudinal force, transverse force and bending moment along the specimen.

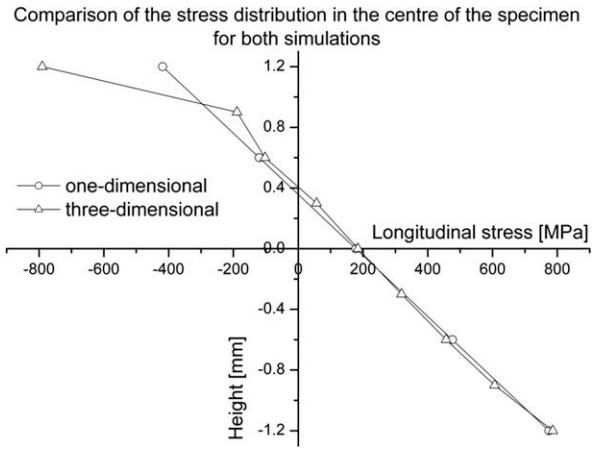


**Fig. 15.** Height distribution of the longitudinal stress in the centre of the specimen.

the specimen increases from 962 to 6280 N. Finally, in Fig. 15, the evolution over the height of the specimen of the longitudinal stress is compared for both the one- as the three-dimensional analysis in the centre of the specimen at a corresponding midspan displacement. It must be remarked that there is an excellent correspondence, except near the top of the specimen, where the three-dimensional analysis yields a higher compressive stress than the one-dimensional. This again proves that the one-dimensional simulation is very useful for the validation of damage models, since there is only a limited deviation in the longitudinal stresses.

## 4. Conclusions

Different bending setups have been discussed for the testing of thin laminate composites. A four-point bending setup has the advantage of being very easily modelled, but the experiments yield low bending forces for large midspan displacements, which only allow low testing frequencies. Inducing membrane stresses by clamping the specimen at the ends on this four-point bending setups yields larger forces for lower displacements, but the failure always occurs next to the clamps, since that is the location of the highest bending moment.

Clamping the ends of the specimen on a three-point bending setup, yields almost four times higher bending loads for less than half the displacement when compared with the regular three-point bending setup. This makes the clamped setup preferable over the unclamped three-point bending. Fatigue tests have also been performed on the clamped setup, with good results.

The validation of damage models can first be done with simple one-dimensional beam theory simulations, but three-dimensional simulations still remain necessary. Further research must be done on how to avoid the slipping in the grips, since this phenomenon certainly has an influence on the measurement.

## Acknowledgements

The authors are highly indebted to the university research fund BOF (Bijzonder Onderzoeksfonds UGent) for sponsoring this research and to Ten Cate Advanced Composites, for supplying the composite material.

## References

[1] Hansen U. Damage development in woven fabric composites during tension–tension fatigue. J Compos Mater 1999;33(7):614–39.
[2] Coats TW, Harris CE. Experimental verification of a progressive damage model for IM7/5260 laminates subjected to tension–tension fatigue. J Compos Mater 1995;29(3):280–305.
[3] Caprino G. Predicting fatigue life of composite laminates subjected to tension–tension fatigue. J Compos Mater 2000;34(16):1334–55.
[4] Gamstedt EK, Sjogren BA. Micromechanisms in tension-compression fatigue of composite laminates containing transverse plies. Compos Sci Technol 1999;59(2):167–78.
[5] Rotem A. The fatigue behaviour of orthotropic laminates under tension-compression loading. Int J Fatigue 1991;13(3):209–15.
[6] Sedrakian A, Ben Zineb T, Billoet JL, Sicot N, Lardeur P. A numerical model of fatigue behaviour for composite plates: application to a three point bending test. In: Degallaix S, Bathias C, Fougères R, editors. International conference on fatigue of composites. Proceedings, 3–5 June 1997, Paris, France, La Société Française de Métallurgie et de Matériaux; 1997. p. 415–23.
[7] Sidoroff F, Subagio B. Fatigue damage modelling of composite materials from bending tests. In: Matthews FL, Buskell NCR, Hodgkinson JM, Morton J, editors. Sixth international conference on composite materials (ICCM-VI) & second European conference on composite materials (ECCM-II): Proceedings, vol 4. 20–24 July 1987. London (UK): Elsevier; 1987. p. 4.32–9.
[8] Caprino G, D'Amore A. Flexural fatigue behaviour of random continuous-fibre-reinforced thermoplastic composites. Compos Sci Technol 1998;58:957–65.
[9] Van Paepegem W, De Geyter K, Vanhooymissen P, Degrieck J. Effect of friction on the hysteresis loops from three-point bending fatigue tests of fibre-reinforced composites. Compos Struct 2006;72(2):212–7.
[10] De Baere I, Van Paepegem W, Degrieck J. On the feasibility of a three-point bending setup for the validation of (fatigue) damage models for thin composite laminates, Polym Compos. doi:org/10.1002/pc.20465.
[11] De Baere I, Van Paepegem W, Degrieck J, Sol H, Van Hemelrijck D, Petreli A. Comparison of different identification techniques for measurement of quasi-zero Poisson's ratio of fabric reinforced laminates. Composites part A 2007;38(9):2047–54.
[12] Young WC, Budynas RG. Roark's formulas for stress and strain, ISBN 0-07-121059-8, McGraw-Hill Compaines Inc.; 7th ed. 2002.